

Electronic Structure and Substitution and Redox Reactivity of Imidazolate-Bridged Complexes of Pentacyanoferrate and Pentaammineruthenium

Alejandro R. Parise, Luis M. Baraldo, and José A. Olabe*,†

Departamento de Química Inorgánica, Analítica y Química Física (Inquimae), Facultad de Ciencias Exactas y Naturales, Universidad de Buenos Aires, Pabellón 2, Ciudad Universitaria, Capital Federal 1428, Republic of Argentina

Received December 6, 1995®

The mixed-valence compound $[(\text{NC})_5\text{Fe}^{\text{II}}-\text{Im}-\text{Ru}^{\text{III}}(\text{NH}_3)_5]^-M_i$, was prepared in solution and as a solid sodium salt from $[\text{Fe}(\text{CN})_5\text{H}_2\text{O}]^{3-}$ and $[\text{Ru}(\text{NH}_3)_5\text{Im}]^{2+}$. The binuclear complex shows two bands at 366 nm ($\epsilon = 3350 \text{ M}^{-1} \text{ cm}^{-1}$) and 576 nm ($\epsilon = 1025 \text{ M}^{-1} \text{ cm}^{-1}$), assigned as LMCT transitions, as well as a near-IR band at 979 nm ($\epsilon = 962 \text{ M}^{-1} \text{ cm}^{-1}$) associated with an intervalence transition. By calculation of the Hush model parameters α^2 and H_{ab} (delocalization and electronic coupling factors, respectively), the complex is defined as a valence-trapped $\text{Fe}^{\text{II}}-\text{Ru}^{\text{III}}$ system; this is confirmed by the measured redox potentials at -0.20 V and 0.30 V , associated with redox processes at the ruthenium and iron center, respectively. The formation stability constant of the mixed-valence ion was obtained through independent measurements of k_f and k_d , the formation and dissociation specific rate constants, respectively. The stabilization of M_i with respect to disproportionation into the isovalent states, as well as toward the formation of the electronic isomer, $\text{Fe}^{\text{III}}-\text{Im}-\text{Ru}^{\text{II}}$, was also estimated. The fully reduced (R_i) and fully oxidized (O_i) binuclear complexes were prepared in solution and characterized by UV–vis spectroscopy. The kinetics of the reactions of R_i and M_i with peroxydisulfate were measured and a mechanistic analysis was performed, showing the relevance of electronic isomerization in completing the full conversion to O_i , through the assistance of the $\text{Ru}^{\text{II}}(\text{NH}_3)_5^{2+}$ center in the oxidation of the neighboring $\text{Fe}^{\text{II}}(\text{CN})_5^{3-}$ moiety. The latter results are compared with those obtained with related complexes comprising different $\text{X}_5\text{M}-\text{L}$ moieties bound to $\text{Ru}^{\text{II}}(\text{NH}_3)_5^{2+}$. A linear correlation is displayed by plotting $\ln k_{\text{et}}$ against E°_{Ru} , associated with the intramolecular oxidation rate constant of Ru^{II} in the ion pair (binuclear species + peroxydisulfate) and the reduction potential of the corresponding $\text{Ru}^{\text{III/II}}$ couple in the ion pair.

Introduction

The structure, stability and redox kinetic properties of mixed-valence compounds of the $[(\text{NC})_5\text{Fe}-\text{L}-\text{Ru}(\text{NH}_3)_5]^n$ series have been studied in recent years for pyrazine (pz),¹ 4,4'-bipyridine (bpy),¹ 1,2-bis(4-pyridyl)ethane (bpa),² cyanide,³ and pyridinecarboxamido (pyCONH)⁴ as bridging ligands. On the other hand, the coordination of imidazole (ImH), and its deprotonated form imidazolate (Im^-), were studied with $\text{Fe}(\text{CN})_5^{n-}$ and $\text{Ru}(\text{NH}_3)_5^{n+}$ as mononuclear species.^{5–12} These low-spin d^6-d^5 systems are good models for mimicking the interaction of porphyrinic metal centers with ImH.^{11–13}

The imidazole ligand is potentially able to bridge between metal ion centers in metalloenzymes; imidazolate bridges exist

in the bovine erythrocyte superoxide dismutase,¹⁴ and a current interest arises on the ability of Im^- to bring about electronic and magnetic interactions between two coordinated metal fragments.¹⁵ A few robust systems were described with bridging Im^- ,¹⁶ and the role of the latter as an electron transfer mediator in intramolecular redox processes was investigated.^{16,17}

We present here the synthesis and characterization of the $[(\text{NC})_5\text{Fe}-\text{Im}-\text{Ru}(\text{NH}_3)_5]^n$ binuclear species, in the mixed-valence (M_i), fully oxidized (O_i), and fully reduced (R_i) forms (the latter two only in solution). We search on the mechanistic features displayed by iron and ruthenium in the oxidation reactions of the binuclear complexes with peroxydisulfate, as was done with related species.¹⁸

Experimental Section

Materials. $[\text{Ru}(\text{NH}_3)_5\text{ImH}]\text{Cl}_3$ and $\text{Na}_3[\text{Fe}(\text{CN})_5\text{NH}_3] \cdot 3\text{H}_2\text{O}$ were prepared according to literature procedures.^{10,19} $[\text{Rh}(\text{NH}_3)_5\text{Im}]\text{Cl}_2$ was prepared by reaction of $\text{Rh}(\text{NH}_3)_5\text{H}_2\text{O}^{3+}$ with ImH (28 h at 120°C , in *N,N*-dimethylacetamide), following the procedure for making $[\text{Rh}(\text{NH}_3)_5\text{pz}](\text{ClO}_4)_3$.²⁰

† Telefax: 54-1-7820441. E-mail: olabe@ayelen.q3.fcen.uba.ar.

® Abstract published in *Advance ACS Abstracts*, May 15, 1996.

- (1) Yeh, A.; Haim, A. *J. Am. Chem. Soc.* **1985**, *107*, 369.
- (2) Olabe, J. A.; Haim, A. *Inorg. Chem.* **1989**, *28*, 3277.
- (3) Burewicz, A.; Haim, A. *Inorg. Chem.* **1988**, *27*, 1611.
- (4) Huang, H. Y.; Chen, W. J.; Yang, C. C.; Yeh, A. *Inorg. Chem.* **1991**, *30*, 1862.
- (5) Shepherd, R. E. *J. Am. Chem. Soc.* **1976**, *98*, 3329.
- (6) Johnson, C. R.; Shepherd, R. E.; Marr, B.; O'Donnell, S.; Dressick, W. J. *J. Am. Chem. Soc.* **1980**, *102*, 6227.
- (7) Toma, H. E.; Batista, A.; Gray, H. B. *J. Am. Chem. Soc.* **1982**, *104*, 7509.
- (8) Johnson, C. R.; Henderson, W. W.; Shepherd, R. E. *Inorg. Chem.* **1984**, *23*, 2754.
- (9) Johnson, C. R.; Shepherd, R. E. *Synth. React. Inorg. Met. Org. Chem.* **1984**, *14*, 339.
- (10) Sundberg, R. J.; Bryan, R. P.; Taylor, I. F.; Taube, H. *J. Am. Chem. Soc.* **1974**, *96*, 381.
- (11) Walters, M. A.; Spiro, T. G. *Inorg. Chem.* **1983**, *22*, 4014.
- (12) Jones, C. M.; Johnson, C. R.; Asher, S. A.; Shepherd, R. E. *J. Am. Chem. Soc.* **1985**, *107*, 3772.
- (13) Sundberg, R. J.; Martin, R. B. *Chem. Rev.* **1974**, *74*, 471.

- (14) (a) Richardson, J. S.; Thomas, K. A.; Rubin, B. H.; Richardson, D. C. *Proc. Natl. Acad. Sci. U.S.A.* **1975**, *72*, 1349. (b) Beem, K. M.; Richardson, D. C.; Rajagopalan, K. V. *Biochemistry* **1977**, *16*, 1930.
- (15) Gross, R.; Kaim, W. *Inorg. Chem.* **1986**, *25*, 4865 and references therein.
- (16) Isied, S. S.; Kuehn, C. G. *J. Am. Chem. Soc.* **1978**, *100*, 6754.
- (17) Szczy, A. P.; Haim, A. *J. Am. Chem. Soc.* **1981**, *103*, 1679.
- (18) Haim, A. *Taube Insights: From Electron Transfer Reactions to Modern Inorganic Chemistry*. *Adv. Chem. Ser.* in press.
- (19) (a) Kenney, D. J.; Flynn, T. P.; Gallini, J. B. *J. Inorg. Nucl. Chem.* **1961**, *20*, 75. (b) Jwo, J. J.; Haim, A. *J. Am. Chem. Soc.* **1976**, *98*, 1172.
- (20) Creutz, C.; Taube, H. *J. Am. Chem. Soc.* **1973**, *95*, 1086.

Isonicotinamide (Aldrich), dimethyl sulfoxide (Baker), and acetone (Mallinckrodt) were used as supplied. Other chemicals (ascorbic acid, potassium nitrate, sodium chloride, and sodium tetraborate decahydrate) were analytical grade reagents. The latter compound was used for buffering, together with NaOH. Deionized, deoxygenated water was used in all of the experiments.

Synthesis of the Binuclear Complexes. The solid compound $\text{Na}[(\text{NC})_5\text{Fe}^{\text{II}}-\text{Im}-\text{Ru}^{\text{III}}(\text{NH}_3)_5]\cdot 6\text{H}_2\text{O}$ was obtained by mixing equimolar solutions of $\text{Na}_3[\text{Fe}(\text{CN})_5\text{NH}_3]\cdot 3\text{H}_2\text{O}$ and $[\text{Ru}(\text{NH}_3)_5\text{ImH}]\text{Cl}_3$ (0.2 mmol in 2 mL), at pH 11.0 (NaOH, unbuffered), under anaerobic conditions; after 20 min, the compound was precipitated by adding deoxygenated acetone and was filtered off and dried over silica gel. Anal. Calcd for $\text{C}_8\text{H}_{30}\text{N}_{12}\text{O}_6\text{FeNaRu}$: C, 16.85; H, 5.30; N, 29.47. Found: C, 17.50; H, 5.13; N, 29.24. The solid was not stable on air exposure; in a few days, signs of decomposition appeared by formation of pieces of black residue. The freshly prepared, dry solid was poorly soluble in water; the suspension and a solution prepared by mixing the mononuclear species in equimolar, dilute conditions (10^{-4} – 10^{-3} M) showed the same electronic spectrum. The latter solutions of the M_i complex were stable up to pH 14 for several hours. The $[\text{Ru}^{\text{III}}(\text{NH}_3)_5\text{Im}]^{2+}$ ion was stable for at least 1 h, up to pH 11.

The fully oxidized dimer, $[(\text{NC})_5\text{Fe}^{\text{III}}-\text{Im}-\text{Ru}^{\text{III}}(\text{NH}_3)_5]$, O_i , was prepared in aqueous solution by mixing a solution of M_i (ca. 10^{-3} M) with a 5-fold excess of a solution of potassium peroxydisulfate. The main brownish product was purified in a Sephadex G-25 column. The solutions of O_i decompose in concentrated media, but the 10^{-4} – 10^{-3} M solutions could be handled for several hours without decomposition, provided that the pH was lower than 10; at higher pH's decomposition ensues in 0.5 h. The binuclear complex O_i was also obtained through a controlled-potential electrochemical synthesis, at $E = +0.45$ V, starting from a 10^{-4} M solution of M_i , at pH 9.5. The complete oxidation process was carried out in successive steps; during each interruption, the rest potential and the electronic spectrum were measured. The experimental data were treated by factor analysis procedures,²¹ by fitting to a one-electron redox process; thus, the standard potential at the iron center, as well as the independent spectra of the pure M_i and O_i complexes, was obtained. In both (chemical and electrochemical) synthetic procedures, the same electronic spectra were obtained for O_i . Also, equal square-wave voltammograms were obtained with solutions of the M_i and O_i complexes.

The fully reduced binuclear complex, R_i , was obtained in aqueous solution by reduction of M_i with amalgamated Zn at pH 14; alternatively, in a complementary experiment as described before, a 10^{-4} M solution of M_i was reduced electrochemically at -0.35 V, pH 10.8.

The model compound $[(\text{NC})_5\text{Fe}^{\text{II}}-\text{Im}-\text{Rh}^{\text{III}}(\text{NH}_3)_5]^-$ was prepared in solution (ca. 10^{-4} M) by mixing equimolar solutions of $\text{Fe}(\text{CN})_5\text{NH}_3^{3-}$ and $\text{Rh}(\text{NH}_3)_5\text{Im}^{2+}$.

Physicochemical Measurements. The infrared spectrum of solid M_i was obtained with a Nicolet 510P FT-IR spectrophotometer, with KBr pellets. Visible–UV and near-IR spectra were measured with Hewlett-Packard 8451A diode array and UV-160A Shimadzu spectrometers, respectively. Electrochemical data were obtained either by cyclic or square-wave voltammetry (the latter technique was more sensitive in 10^{-4} M solutions), with a Princeton Applied Research 273A potentiostat, by using a cell with a standard three-electrode configuration; a specially designed cell was employed for the spectroelectrochemical experiments. The solutions were deoxygenated during all the experiments. The potentials are reported vs NHE. The stopped-flow kinetic measurements were performed with a Hi-Tech PQ/SF-53 spectrophotometer.

Kinetic and Equilibrium Studies. The kinetics of the formation reaction of M_i was followed in stopped-flow conditions by a competitive method,²² by mixing deoxygenated solutions of freshly generated $\text{Fe}(\text{CN})_5\text{H}_2\text{O}^{3-}$ (by rapid aquation of $\text{Fe}(\text{CN})_5\text{NH}_3^{3-}$, pH 6.0, $c = 10^{-4}$ M)²³ with buffered solutions of $\text{Ru}(\text{NH}_3)_5\text{Im}^{2+}$ (pH 10.8) in the concentration range $(1-5) \times 10^{-3}$ M. The latter solutions contained

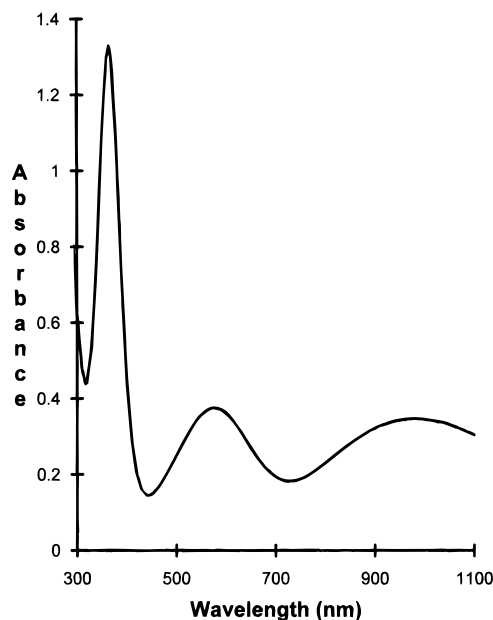


Figure 1. Absorption spectrum of $[(\text{NH}_3)_5\text{Fe}^{\text{II}}-\text{Im}-\text{Ru}^{\text{III}}(\text{NH}_3)_5]^-$ (M_i) ($c = 3.9 \times 10^{-4}$ M; pH = 11.6; $I = 0.1$ M; $T = 25^\circ\text{C}$).

a fixed amount of isonicotinamide (isn), 10^{-3} M. The final ionic strength was 0.1 M (NaCl). The measurements were performed at 435 nm, the absorbance maximum of the competitive product, $\text{Fe}(\text{CN})_5\text{isn}^{3-}$.²⁴ Pseudo-first-order rate constants, k_{obs} , were obtained by plotting $\ln[A_\infty - A_t]$ vs time (A_∞ and A_t are the absorbances at the completion of reaction and at time t , respectively). A good linear behavior was observed, up to 3 half-lives. From the linear plot of k_{obs} against the concentration of $\text{Ru}(\text{NH}_3)_5\text{Im}^{2+}$, the specific second-order rate constant, k_f , was obtained (25°C). The same value of k_f was obtained by mixing equimolar 10^{-4} M solutions of the mononuclear reactants, with a direct measurement of the absorbance increase at 820 nm; the data were treated by fitting to a second-order reaction scheme.

The kinetics of the dissociation reaction of M_i were measured by mixing a solution of the freshly generated dimer M_i (10^{-4} M) in a slight excess of $\text{Ru}(\text{NH}_3)_5\text{Im}^{2+}$ (3×10^{-4} M), with a solution of a scavenger ligand, isonicotinamide, in a high excess (range 0.1–1 M). The measurements were carried out at pH 10.8, $I = 0.1$ M (KNO_3), $T = 25^\circ\text{C}$, by following the increase of absorbance of $\text{Fe}(\text{CN})_5\text{isn}^{3-}$, at 435 nm. The data were treated under pseudo-first-order conditions, in a similar way as for the formation reaction. A complementary experiment was done by using dimethyl sulfoxide (dmsO) as a scavenger ligand and by following the decrease of absorption at 820 nm.

The kinetics of the redox conversion of M_i (10^{-4} M)²⁵ into O_i by reaction with peroxydisulfate (range $(5-10) \times 10^{-3}$ M) was followed under stopped-flow conditions (pH 10.8, $I = 0.1$ M, KNO_3), by measuring the absorbance increase of the product at 470 nm or, alternatively, the decrease at 820 nm (tail of the intervalence band of the reactant). The reaction of the model compound $[(\text{NC})_5\text{Fe}^{\text{II}}-\text{Im}-\text{Rh}^{\text{III}}(\text{NH}_3)_5]^-$ with peroxydisulfate was studied by conventional spectrophotometry, by following the increase of absorbance of the product at 406 nm, in similar conditions as in the reaction of the M_i compound.

The stability constant of the M_i complex, K_{eq} , was obtained by using independently measured values of k_f and k_d , the specific formation and dissociation rate constants, respectively.

Results and Discussion

Spectral and Electrochemical Characterization of the Imidazolate-Bridged Complexes, M_i , O_i , and R_i . When solid

(24) Toma, H. E.; Malin, J. M. *Inorg. Chem.* **1973**, *12*, 1039.

(25) A 10^{-2} M solution of M_i was diluted to 10^{-4} M and made to react rapidly with peroxydisulfate, thus avoiding the presence of significant amounts of $\text{Ru}(\text{NH}_3)_5\text{Im}^{2+}$ (the $\text{Ru}(\text{III})$ mononuclear species may catalyze the oxidation reaction of M_i through an intermolecular path; see below).

(21) Parise, A. R.; Pollak, S.; Slep, L. D.; Olabe, J. A. *An. Asoc. Quim. Argent.* **1995**, *83*, 211.

(22) Toma, H. E.; Malin, J. M.; Giesbrecht, E. *Inorg. Chem.* **1973**, *12*, 2084.

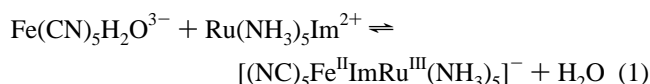
(23) Toma, H. E.; Malin, J. M. *Inorg. Chem.* **1974**, *13*, 1772.

Table 1. Electronic Transitions in nm (ϵ in $\text{M}^{-1} \text{cm}^{-1}$) in Mononuclear and Binuclear Imidazolate Complexes with $\text{Fe}(\text{CN})_5$ and $\text{Ru}(\text{NH}_3)_5$

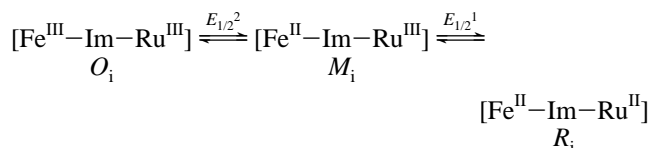
	$(\pi_{1L})^a \rightarrow d\pi(\text{M}^{\text{III}})$	$(\pi_{2L})^a \rightarrow d\pi(\text{M}^{\text{III}})$	$(\text{CN}^-) \rightarrow d\pi(\text{Fe}^{\text{III}})$	d-d	E° ^b
$[\text{Fe}^{\text{III}}(\text{CN})_5\text{ImH}]^{2-}$	475 (376) ^{c,d}	403 (1180) ^{c,d}	356 (981), ^{c,d} 293 (1800) ^d		0.365, ^d 0.34 ^e
$[\text{Fe}^{\text{III}}(\text{CN})_5\text{Im}]^{3-}$	625(400) ^d	438 ^c (2100) ^d	360 ^f (950), ^d 290 (1350) ^d		
$[\text{Ru}^{\text{III}}(\text{NH}_3)_5\text{ImH}]^{3+}$	425, ^b 430 (250) ^g	297, ^c 255 ^c			0.11 ^h
$[\text{Ru}^{\text{III}}(\text{NH}_3)_5\text{Im}]^{2+}$	550 ^c (380)	360 ^c (3050), 245 ^c sh (970)			0.03
$[\text{Fe}^{\text{II}}(\text{CN})_5\text{ImH}]^{3-}$				383 (430) ^e	
$[\text{Ru}^{\text{II}}(\text{NH}_3)_5\text{ImH}]^{2+}$				255 (2800), ^g 280 (2700) ^g	
$[(\text{NC})_5\text{Fe}^{\text{II}}\text{ImRu}^{\text{III}}(\text{NH}_3)_5]^-$	576(1025)	366 (3350)			-0.20
$[(\text{NC})_5\text{Fe}^{\text{III}}\text{ImRu}^{\text{III}}(\text{NH}_3)_5]^0$	458 (2200) (Fe); 400 (2600), sh (Ru)	356 (3400) ⁱ	356 (3400), 286 (2100) ^j		0.30 ^j
$[(\text{NC})_5\text{Fe}^{\text{II}}\text{ImRu}^{\text{II}}(\text{NH}_3)_5]^{2-}$				390 (524), br	

^a The (π_{1L}) orbital has more electron density at the carbon atoms, and the (π_{2L}) orbital has more electron density at the nitrogen atoms. The n orbital corresponds to the pyridine-like nitrogen (cf. ref 12). ^b Volts vs NHE, $I = 0.1 \text{ M}$. ^c References 8 and 12. ^d Reference 5. ^e Reference 7. ^f Reference 11. ^g Reference 10. Assignments in Ru(II) complexes are suggested by us. ^h Reference 26. ⁱ Tentative assignments. ^j Reduction of iron.

$\text{Na}_3[\text{Fe}(\text{CN})_5\text{NH}_3] \cdot 3\text{H}_2\text{O}$ is added to a solution of $\text{Ru}(\text{NH}_3)_5\text{-Im}^{2+}$ (in equimolar conditions, buffered in the pH range 10–13), under argon, definite spectral changes are observed in the minute time scale. Two bands appear at 366 nm ($\epsilon = 3350 \text{ M}^{-1} \text{cm}^{-1}$) and 576 nm ($\epsilon = 1025 \text{ M}^{-1} \text{cm}^{-1}$) in the visible region. In addition, a band at 979 nm ($\epsilon = 962 \text{ M}^{-1} \text{cm}^{-1}$, corrected for the presence of mononuclear species in equilibrium) shows up in the near-IR region (Figure 1). We propose that the binuclear complex M_i is formed, according to eq 1, following aquation of the $\text{Fe}(\text{CN})_5\text{NH}_3^{3-}$ ion.



At the experimental pH, deprotonation of coordinated ImH ensues (pK_a of $\text{Ru}^{\text{III}}(\text{NH}_3)_5\text{ImH}^{3+} = 8.9$)¹⁰ and bridging to $\text{Fe}(\text{CN})_5\text{H}_2\text{O}^{3-}$ is feasible. An electrochemical experiment shows that the initial peak at 0.03 V (measured by us, corresponding to reduction of $[\text{Ru}^{\text{III}}(\text{NH}_3)_5\text{Im}]^{2+}$)⁹ decreases in intensity through the successive addition of $\text{Fe}(\text{CN})_5\text{NH}_3^{3-}$, while new peaks appear at -0.20 V ($E_{1/2}^1$) and 0.30 V ($E_{1/2}^2$), associated to the formation of the M_i complex. We assign the peaks as follows:



From the electronic spectrum and electrochemical results, we describe M_i as a mixed-valence species featuring Fe^{II} and Ru^{III} localized sites. We assign the visible bands to LMCT transitions from Im^- to $\text{Ru}(\text{III})$; both are slightly shifted to lower energies compared to those in the mononuclear $\text{Ru}(\text{NH}_3)_5\text{Im}^{2+}$ ion (Table 1). The shifts are consistent with the π -donor influence of $\text{Fe}(\text{CN})_5^{3-}$, which destabilizes the filled π -orbitals of Im^- in the binuclear species. The rising absorption below 300 nm corresponds to $d\pi \rightarrow \pi^*(\text{CN})$ MLCT transitions. No band assignable to a $d\pi \rightarrow \pi^*(\text{Im}^-)$ MLCT transition is detected in the near-UV-visible region. The d-d band associated with the iron center is most probably buried under the intense 366 nm band (it was assigned at 382 nm in $\text{Fe}(\text{CN})_5\text{ImH}^{3-}$ ion).⁵ Finally, we assign the band at 979 nm to the intervalence (IV) transition, from $\text{Fe}(\text{II})$ to $\text{Ru}(\text{III})$. On the basis of the reduction potentials, the latter configuration should be highly predominant over the one for the electronic isomer, M'_i , featuring Fe^{III} and Ru^{II} sites (see below).

The reduction potential at the ruthenium site is more negative in the binuclear species than in the mononuclear $\text{Ru}^{\text{III}}(\text{NH}_3)_5\text{-ImH}^{3+}$ ion;²⁶ the imidazolate ligand acts as a stronger electron

donor than ImH and shifts electron density onto the ruthenium center; besides, the coordination of $\text{Fe}(\text{CN})_5^{3-}$ reinforces the effect (the influence of π -donors in lowering the Ru potential when coordinating to the exposed end of a biphilic ligand has been discussed elsewhere).¹ On the other hand, the potentials associated with the iron centers in $\text{Fe}^{\text{II}}(\text{CN})_5\text{ImH}^{3-}$ and in the binuclear complex are similar,⁹ thus suggesting that the influence of the proton on coordinating to Im^- is comparable to that from the $\text{Ru}^{\text{III}}(\text{NH}_3)_5^{3+}$ moiety. The iron potentials are lower than those found for the $\text{Fe}^{\text{III,II}}(\text{CN})_5\text{H}_2\text{O}^{2-/3-}$ couple, 0.36 V ($I = 0.1 \text{ M}$);²¹ this fact, together with the absence of MLCT transitions, indicates a negligible π -acceptor ability of Im^- in the binuclear complex.

The IR spectrum of the solid mixed-valence complex is in agreement with the previous assignments, showing bands at 2039 and 1327 cm^{-1} (associated with cyanide-stretching and ammonia deformation, respectively); both are diagnostic of $\text{Fe}(\text{II})$ and $\text{Ru}(\text{III})$, respectively.^{1,2} Besides, other bands from imidazole and ammonia are present, in correspondence to those measured in $[\text{Ru}(\text{NH}_3)_5\text{ImH}]\text{Cl}_3$.

The properties of the IV band, as well as the parameters obtained through the application of theoretical treatments,²⁷ are displayed in Table 2, together with the results for related imidazolate-bridged binuclear complexes and species with other L-bridging ligands of the pentacyanoferrate-L-pentaammineruthenium series. The results for $L = \text{Im}^-$ are consistent with the proposed valence-trapped formulation, as shown by α^2 and H_{ab} values (the delocalization parameter and the electronic coupling factor, respectively), as well as from the comparison of calculated and measured bandwidths.^{27,28} In spite of the nonlinear configuration of the $[\text{Fe}^{\text{II}}\text{-Im-Ru}^{\text{III}}]$ unit, the latter shows the highest value of H_{ab} ; thus, Im^- behaves as a good electron-communicating ligand, similar to pyrazine, probably because of its small dimensions. The mechanism of electronic conduction through the bridge is probably of the "hole-transfer" type, rather than of "electron-transfer" type.²⁹ The latter interaction is established in the complexes with pyrazine and other bridging ligands with low-energy empty π^* orbitals, but this is evidently not the case with imidazolate, as shown above. On the other hand, the hole-transfer mechanism could be favored by the more efficient energy match of the $d\pi$ metal orbitals and the occupied π -orbitals of the imidazolate bridge; this has been shown to be the case for some binuclear complexes with

(26) Kuehn, C. G.; Taube, H. *J. Am. Chem. Soc.* **1976**, *98*, 689.

(27) Hush, N. S. *Prog. Inorg. Chem.* **1967**, *8*, 391.

(28) Creutz, C. *Prog. Inorg. Chem.* **1983**, *30*, 1.

(29) (a) Giuffrida, G.; Campagna, S. *Coord. Chem. Rev.* **1994**, *135/136*, 517. (b) Hage, R.; Haasnoot, J. G.; Reedijk, J.; Vos, J. G. *Chemtracts-Inorg. Chem.* **1992**, *4*, 75.

Table 2. Theoretical Calculations in Intervalence Dimers (Hush Model)

	λ_{\max} (nm)	ν_{\max} (10^3 cm^{-1})	ϵ_{\max} ($\text{M}^{-1} \text{ cm}^{-1}$)	$\Delta\nu_{1/2}(\text{calc}; \text{exp})$ (cm^{-1}) ^a	H_{ab} (cm^{-1}) ^b	α^2 ^c	ref
$[(\text{NC})_5\text{Fe}^{\text{II}}-\text{Im}-\text{Ru}^{\text{III}}(\text{NH}_3)_5]^-$	979	10.2	962	4100; 5000	756 ^d	5.4×10^{-3}	this work
$[(\text{NH}_3)_5\text{Ru}^{\text{II}}-\text{Im}-\text{Ru}^{\text{III}}(\text{NH}_3)_4(\text{SO}_4)]^{2+}$	1375	7.3	1000	-; 4300 ^e	602 ^f	6.8×10^{-3}	17
$[(\text{NC})_5\text{Fe}^{\text{II}}-\text{Pz}-\text{Ru}^{\text{III}}(\text{NH}_3)_5]^0$	1650	6.1	1550	3700; 4300	600	9.8×10^{-3}	1
$[(\text{NC})_5\text{Fe}^{\text{II}}-\text{PyCONH}-\text{Ru}^{\text{III}}(\text{NH}_3)_5]^-$	645	15.5	570	5100; 5100	480	9.5×10^{-4}	4

^a Calculated from $\Delta\nu_{1/2} = [2319(\nu_{\max} - \Delta E^{\circ}_{\text{et}})]^{1/2}$.²⁷ ^b Calculated from $H_{\text{ab}} = 2.02 \times 10^{-2} (\epsilon_{\max} \Delta\nu_{1/2} / \nu_{\max})^{1/2} \nu_{\max} / r$, with r in Å.²⁷ ^c Calculated from $\alpha^2 = (H_{\text{ab}} / \nu_{\max})^2$.²⁷ ^d $r = 6.06$ Å, obtained by adding 0.06 (difference in radii between Co^{III} and Ru^{III}) to the intermetallic distance in $[(\text{NC})_5\text{Fe}^{\text{II}}\text{ImCo}^{\text{III}}(\text{NH}_3)_5]^-$ (cf. ref 17). ^e Estimated from the spectrum in ref 16. ^f $r = 6.06$ Å; as in footnote d, comparing with $[(\text{NH}_3)_4(\text{H}_2\text{O})\text{Ru}^{\text{II}}\text{ImCo}^{\text{III}}(\text{NH}_3)_5]^{4+}$.¹⁷

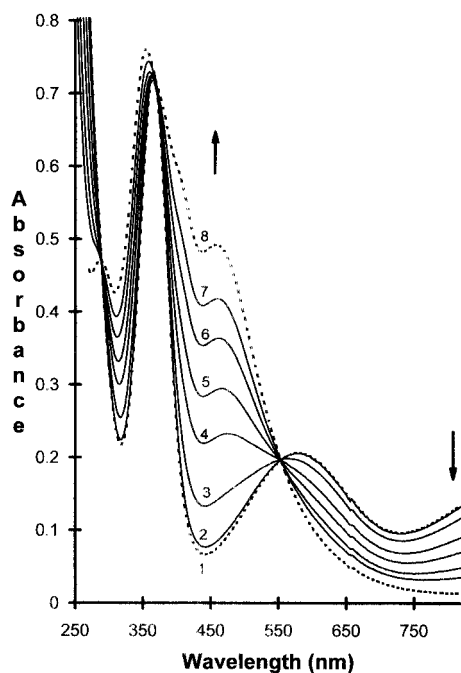


Figure 2. Spectroelectrochemical oxidation of $[(\text{NH}_3)_5\text{Fe}^{\text{II}}-\text{Im}-\text{Ru}^{\text{III}}(\text{NH}_3)_5]^-$ (M_i) to $[(\text{NH}_3)_5\text{Fe}^{\text{III}}-\text{Im}-\text{Ru}^{\text{III}}(\text{NH}_3)_5]$ (O_i) ($c = 2.25 \times 10^{-4}$ M; pH = 9.5; $I = 0.1$ M; $T = 25$ °C). Spectra 2–7 correspond to partially electrolyzed mixtures with increasing percentage of O_i (rest potentials 0.190, 0.247, 0.277, 0.294, 0.313, and 0.332 V (NHE), respectively). Spectra 1 and 8 correspond to pure M_i and O_i , respectively, obtained by factor analysis.

deprotonated bibenzimidazoles as bridging ligands³⁰ and is probably also operative with bridging cyanide.

Figure 2 show the spectra obtained under controlled potential oxidation, starting from M_i . The isosbestic points at 554 and 288 nm indicate a net transformation to a species presently defined as O_i . It can be seen that the absorption at 820 nm (tail of the IV band) and the band at 576 nm disappear; the original band at 366 nm in M_i shifts to 356 nm. The LMCT bands from the π_1 level of imidazolate are assigned by comparison with those measured in the M^{III} mononuclear species (Table 1). The LMCT bands to Fe(III) are found at lower energies than to Ru(III), because of the stronger oxidizing ability of the iron moiety;⁸ it can also be seen that the maximum wavelengths decrease in the $\text{Fe}^{\text{III}}(\text{CN})_5\text{L}^{n-}$ series in the following order: $\text{L} = \text{Im}^-$ (625 nm) > ImH (480 nm) > $\text{ImRu}^{\text{III}}(\text{NH}_3)_5^{2+}$ (450 nm). The same is observed for the $\text{Ru}^{\text{III}}(\text{NH}_3)_5\text{L}^{n+}$ complexes: Im^- (550 nm) > ImH (430 nm) > $\text{ImFe}^{\text{III}}(\text{CN})_5^{3-}$ (400 nm). The trends are consistent with the decreasing electron-donor ability of the L moiety. The bands at 356 and 288 nm in O_i cannot be unambiguously assigned from simple comparisons; both are also present in the mononuclear Fe(III)

and Ru(III) species (Table 1). The O_i complex can be further reduced to the M_i species with ascorbic acid or through an electrochemical reduction; in any case, the intensities of the M_i bands are recovered up to ca. 80%.

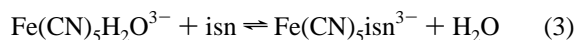
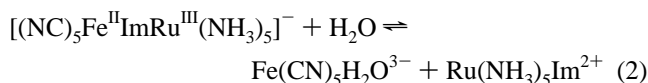
In the spectra obtained under controlled potential reduction (Supporting Information), starting from M_i , all of the M_i bands disappear and a broad absorption obtains at 350–500 nm. From the equilibrium and redox potential data, we predict that R_i must dissociate significantly into the mononuclear species, $\text{Fe}(\text{CN})_5\text{H}_2\text{O}^{3-}$ and $\text{Ru}^{\text{II}}(\text{NH}_3)_5\text{ImH}^{2+}$. In fact, the broad feature is in agreement with the presence of $\text{Fe}(\text{CN})_5\text{H}_2\text{O}^{3-}$ ($\lambda_{\max} = 440$ nm),⁷ $\text{Fe}(\text{CN})_5\text{NH}_3^{3-}$ ($\lambda_{\max} = 395$ nm),⁷ and the R_i complex, which should expectedly show a d–d band at ca. 380 nm, as found for $\text{Fe}(\text{CN})_5\text{ImH}^{3-}$.⁵ The bands of M_i are also recovered to ca. 80% by leaving the reduced mixture in an aerated medium or by electrooxidation.

Kinetics and Mechanism of the Formation and Dissociation Reactions of M_i . The rate constants in eq 1 were measured independently. The forward reaction obeys the following rate law:

$$v = d[M_i]/dt = k_f[\text{Ru}(\text{NH}_3)_5\text{Im}^{2+}][\text{Fe}(\text{CN})_5\text{H}_2\text{O}^{3-}]$$

Here, $k_f = (1.8 \pm 0.1) \times 10^3 \text{ M}^{-1} \text{ s}^{-1}$ (25 °C, $I = 0.1$ M, KNO_3). This value is consistent with those obtained for the entry of other members of the $\text{Ru}(\text{NH}_3)_5\text{L}^{2+}$ series ($\text{L} = \text{pz}$, bpy , bpa) into $\text{Fe}(\text{CN})_5\text{H}_2\text{O}^{3-}$ and supports an ion pair-dissociative mechanism for the formation of M_i . The values of k_f in these reactions are dependent on the charges of the entering L ligands into $\text{Fe}(\text{CN})_5\text{H}_2\text{O}^{3-}$;³¹ thus, a significantly lower value, $240 \text{ M}^{-1} \text{ s}^{-1}$, was found for the entry of neutral ImH .³²

The kinetics of dissociation of M_i (reverse reaction in eq 1) was studied by reacting M_i with a scavenger ligand for the $\text{Fe}(\text{CN})_5\text{H}_2\text{O}^{3-}$ initial product, according to eqs 2 and 3.



The experimental rate law was $v = -d[M_i]/dt = k_{\text{obs}}[M_i]$, with k_{obs} being independent of the nature of the scavenger used. Assuming that saturation conditions are operative, k_{obs} is equal to $k_d = k_{-\text{Ru}(\text{NH}_3)_5\text{Im}}$, the specific dissociation rate constant for the cleavage of the Fe–Im bond. For reaction 2, $k_d = 1.00 \times 10^{-3} \text{ s}^{-1}$ (25 °C, $I = 0.1$ M), a value very similar to the dissociation of ImH from $\text{Fe}(\text{CN})_5\text{ImH}^{3-}$, $k_{-\text{ImH}} = 1.33 \times 10^{-3} \text{ s}^{-1}$.⁷ The results support a dissociative mechanism, as generally accepted in $\text{Fe}(\text{CN})_5\text{L}^{n-}$ systems.^{24,31} The first, slow step in the mechanism (eq 2) is the dissociation of the L ligand (namely

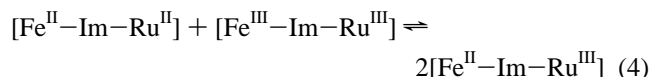
(31) Macartney, D. H. *Rev. Inorg. Chem.* **1988**, 9, 101.

(32) Toma, H. E.; Martins, J. M.; Giesbrecht, E. *J. Chem. Soc., Dalton Trans.* **1978**, 1610.

(30) Haga, M.; Ano, T.; Kano, K.; Yamabe, S. *Inorg. Chem.* **1991**, 30, 3843.

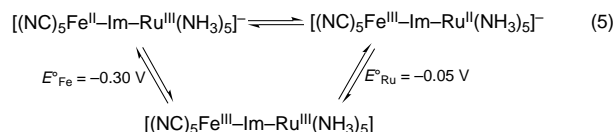
the $\text{Ru}(\text{NH}_3)_5\text{Im}^{2+}$ ion), followed by rapid coordination of the scavenger into $\text{Fe}(\text{CN})_5\text{H}_2\text{O}^{3-}$ (eq 3).

Thermodynamic Stability of M_i . The value of K_{eq} for reaction 1 is $1.8 \times 10^6 \text{ M}^{-1}$, showing that M_i is a robust binuclear species, of comparable stability with other members of the series.¹⁻⁴ The difference of potentials between the first and the second redox process, $\Delta E = E_{1/2}^2 - E_{1/2}^1$, is related to the comproportionation constant,³³ K_{com} , eq 4.



The high stability of M_i with respect to the isovalent states ($K_{\text{com}} = 2.8 \times 10^8$, 5.4 kcal/mol) can be traced in a minor degree to the electronic delocalization factor ($\alpha^2\nu_{\text{max}} = 0.12 \text{ kcal/mol}$) as well as to electrostatic factors associated to the net charges of the moieties that make up the binuclear complexes in eq 4; the latter factor also stabilizes the mixed-valence state with respect to the isovalent states, by ca. 1 kcal/mol.¹ Thus, the main stabilizing factor can be associated with $d\pi-\pi$ interactions. In contrast to the analogous pyrazine-bridged complex, where $d\pi-\pi^*$ back-bonding is operative,¹ now the mixed-valence complex is stabilized by the π -donor(Im^-)-acceptor(Ru^{III}) interaction, which is reinforced by the π -donor ability of $\text{Fe}^{\text{II}}(\text{CN})_5^{3-}$. In the isovalent II,II state, both $\text{M}^{\text{II}}\text{X}_5$ moieties, as well as Im^- , act as π -donors; on the other hand, in the isovalent III,III state, the acceptor $\text{M}^{\text{III}}\text{X}_5$ moieties compete for the π -donor ability of the imidazolate bridge.

Next, we consider the stability of M_i with respect to its electronic isomer, M_i' , by using a thermodynamic cycle:

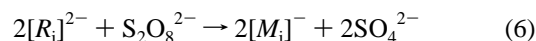


E_{Fe}° is the measured potential for oxidation at the iron site close to a neighboring Ru^{III} site; E_{Ru}° is estimated by comparison with a series of related complexes.³⁴ Thus, $\Delta E_{\text{et}}^\circ = -0.35 \text{ V}$. The greater stability of the $[\text{Fe}^{\text{II}}-\text{Im}-\text{Ru}^{\text{III}}]$ isomer is evidently associated to the stronger oxidizing ability of the $[\text{Fe}^{\text{III}}(\text{CN})_5\text{Im}]^{3-}$ complex compared to $[\text{Ru}^{\text{III}}(\text{NH}_3)_5\text{Im}]^{2+}$.

The M_i dimer is stable for some hours in the pH range 9.5–14, in a deoxygenated medium; at lower pH, a decomposition process ensues. The nature and rate of the overall process depend on pH and concentration of M_i but are not presently well understood. One of the products appears to be the O_i dimer, thus suggesting that an acid-catalyzed disproportionation reaction is operative. Interestingly, the reaction is reversible if pH's lower than 5 are not attained, and thus M_i is regenerated by shifting back the pH to values higher than 9. The results can be related to those described for the dissociation of ImH from the $\text{Fe}(\text{CN})_5\text{ImH}^{3-}$ ion at pH 5⁶ and are probably associated with the competition of H^+ and $\text{Fe}(\text{CN})_5^{3-}$ toward the electron pair in ImH ($\text{p}K_a = 7.06$ for ImH_2^+).¹³ An acid-dependent decomposition was also observed for the $[\text{SO}_4(\text{NH}_3)_4-\text{Ru}^{\text{III}}-\text{Im}-\text{Ru}^{\text{III}}(\text{NH}_3)_5]^{3+}$ mixed-valence species.¹⁶ Acid ca-

talysis could also be the determinant of the faster rate of dissociation of ImH compared to pyridine (by a factor of 10^3) from the respective $\text{Ru}(\text{NH}_3)_5\text{L}^{n+}$ species.¹⁰

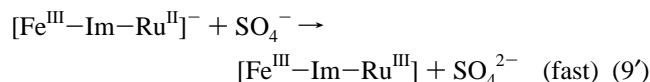
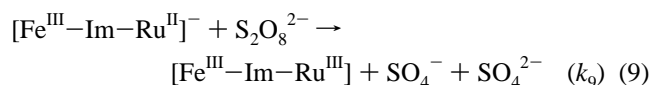
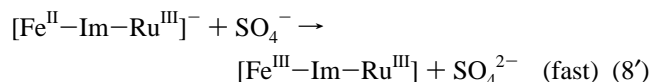
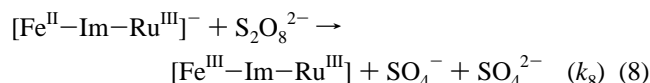
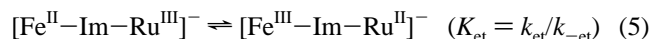
Redox Reactions of R_i and M_i with Peroxydisulfate. When R_i reacts with 1 equiv of peroxydisulfate, the product is the M_i complex, according to the stoichiometry shown in eq 6. The



reaction is very fast, out of the time scale of the stopped-flow technique.³⁵ If an excess of peroxydisulfate is made to react with R_i , the fast process is followed by a slower, measurable reaction, whose product is the O_i dimer (eq 7).

Two possibilities exist for reaction 6 as to the site of attack of peroxydisulfate, namely oxidation at the Fe^{II} site or at the Ru^{II} site. We predict, on the basis of thermodynamic and kinetic considerations, that the Ru^{II} site is the preferential site of oxidation; this is in fact observed,³⁵ as was with similar complexes of the $[(\text{NC})_5\text{Fe}^{\text{II}}-\text{L}-\text{Ru}^{\text{II}}(\text{NH}_3)_5]^-$ series ($\text{L} = \text{pz}$, bpa).^{1,2} We anticipate, on the basis of theoretical predictions³⁶ and the potential at the Ru^{II} site in R_i , $E_{1/2}^1 = -0.20 \text{ V}$, that the rate of oxidation at the ruthenium center should be near the diffusion-controlled limit (see below).

The rate law for reaction 7 was $-d[M_i]/dt = k_{\text{obs}}[M_i]$; a linear plot with zero intercept was obtained by plotting k_{obs} (s^{-1}) against the concentration of peroxydisulfate; from the slope, a value of $k_{2\text{nd}} = 42 \text{ M}^{-1} \text{ s}^{-1}$ (25 °C) was obtained for the specific second-order rate constant. We propose the following reaction scheme:



By applying the steady-state approximation, we obtain the following rate law for the disappearance of M_i :

$$k_{\text{obs}} = 2k_{\text{et}}k_9[\text{S}_2\text{O}_8^{2-}]/(k_{-\text{et}} + 2k_9[\text{S}_2\text{O}_8^{2-}]) + 2k_8[\text{S}_2\text{O}_8^{2-}]$$

If $[\text{S}_2\text{O}_8^{2-}]$ is low enough, the observed rate will be equal to $(2K_{\text{et}}k_9 + 2k_8)[\text{S}_2\text{O}_8^{2-}]$, where $K_{\text{et}} = k_{\text{et}}/k_{-\text{et}}$. At higher $[\text{S}_2\text{O}_8^{2-}]$, k_{obs} will equal $k_{\text{et}} + 2k_8[\text{S}_2\text{O}_8^{2-}]$. From experimental results, we consider that the first limiting conditions are met at the used concentrations of $[\text{S}_2\text{O}_8^{2-}]$ and, therefore, $k_{2\text{nd}} = 2K_{\text{et}}k_9 + 2k_8$.

We can estimate a value for k_8 by considering the reaction of the model compound $[(\text{NC})_5\text{Fe}^{\text{II}}-\text{Im}-\text{Rh}^{\text{III}}(\text{NH}_3)_5]^-$ with

(33) Richardson, D. E.; Taube, H. *Coord. Chem. Rev.* **1984**, *60*, 107.

(34) By considering the species ImH_2^+ , $\text{Fe}^{\text{III}}(\text{CN})_5\text{ImH}_2^+$, and $\text{Fe}^{\text{II}}(\text{CN})_5\text{ImH}^{3-}$, we can use the $\text{p}K_a$ data (7.1, ref 13; 10.5, ref 5; ca. 14, respectively) to estimate the relative electron-withdrawing abilities of the corresponding moieties toward ImH . By the replacement of H by the $\text{Ru}^{\text{III}}(\text{NH}_3)_5^{3+}$ moiety in the above series, reduction potentials at the Ru site have been measured for $\text{Ru}^{\text{III}}(\text{NH}_3)_5\text{ImH}^{3+}$ (0.11 V, ref 26) and for $[(\text{NC})_5\text{Fe}^{\text{II}}\text{ImRu}^{\text{III}}(\text{NH}_3)_5]^-$ (-0.20 V, this work). By interpolating in the linear correlation of E_{Ru}° against $\text{p}K_a$, we estimate $E = -0.05 \text{ V}$ for the reduction at $[(\text{NC})_5\text{Fe}^{\text{III}}\text{ImRu}^{\text{III}}(\text{NH}_3)_5]$.

(35) The experiment showing the conversion $R_i \rightarrow M_i$ was performed qualitatively, by mixing equimolar amounts of R_i and peroxydisulfate; as the R_i complex is unstable, the mixture contains significant amounts of the mononuclear species. However, an unmeasurable rising trace was observed at 820 nm, followed by a slower decay (conversion $M_i \rightarrow O_i$).

(36) Haim, A. *Comments Inorg. Chem.* **1985**, *4*, 113.

Table 3. Experimental and Corrected Values for Rate Constants^a and Redox Potentials at the Ru Site in the [X₅M–L–Ru^{III,II}(NH₃)₅]ⁿ Series

no.	[X ₅ M–L] ^{n–}	exptl values			corrected values			ref
		<i>E</i> ^o _{Ru} /V	<i>k</i> _{2nd} /M ^{–1} s ^{–1}	ln <i>k</i> _{2nd}	<i>E</i> ^o _{Ru} /V ^b	<i>k</i> _{et} ^c /s ^{–1}	ln <i>k</i> _{et}	
1	(NC) ₅ Fe ^{III} –Im ^{3–}	–0.05	1.71 × 10 ⁷	16.65	–0.087	1.25 × 10 ⁸	18.64	this work
2	(NC) ₅ Fe ^{II} –bpa ^{3–}	0.290	5.00 × 10 ⁴	10.82	0.253	3.66 × 10 ⁵	12.81	2
3	(NC) ₅ Fe ^{III} –bpa ^{2–}	0.290	1.50 × 10 ⁵	11.92	0.235	2.62 × 10 ⁵	12.48	2
4	(edta)Ru ^{II} –pz ^{2–}	0.410	2.50 × 10 ⁴	10.13	0.355	4.37 × 10 ⁵	10.69	37
5	(NC) ₅ Fe ^{II} –pz ^{3–}	0.490	3.79 × 10 ³	8.24	0.453	2.77 × 10 ⁴	10.23	1
6	(NC) ₅ Fe ^{II} –3pyCN ^{3–}	0.550	7.20 × 10 ²	6.58	0.513	5.30 × 10 ³	8.58	38
7	(NC) ₅ Fe ^{II} –4pyCN ^{3–}	0.550	6.20 × 10 ²	6.43	0.513	4.54 × 10 ³	8.42	38
8	(NC) ₅ Fe ^{III} –3pyCN ^{2–}	0.600	6.30 × 10 ²	6.45	0.545	1.10 × 10 ³	7.00	38
9	(NC) ₅ Co ^{III} –pz ^{2–}	0.655	1.40 × 10 ²	4.94	0.600	2.50 × 10 ²	5.52	1
10	(NC) ₅ Fe ^{III} –4pyCN ^{2–}	0.660	3.70 × 10 ²	5.91	0.605	6.50 × 10 ²	6.48	38

^a Corresponds to reaction 10; see text. ^b Corresponds to the redox potential within the ion pair. The corrections were done by considering *K*_{ip} values for the formation and dissociation of the precursor and successor complexes, respectively (cf. ref 39). ^c *k*_{et} = *k*_{2nd}/*K*_{ip}; *K*_{ip} was calculated according to ref 36, by taking radii for Ru(NH₃)₅²⁺ and S₂O₈^{2–} as given in refs 39 and 40, respectively.

peroxydisulfate. We found the same rate law as with *M*_i, with *k*'_{2nd} = 1 M^{–1} s^{–1}; thus, we calculate 2*K*_{et}*k*₉ = 41 M^{–1} s^{–1}. By using Δ*E*^o_{et} = –0.35 V (eq 5), we obtain *K*_{et} = 1.2 × 10^{–6} and *k*₉ = 1.71 × 10⁷ M^{–1} s^{–1}. It can be seen that a more efficient path is open for reaction of *M*_i with peroxydisulfate, in addition to reaction 8, through the rapid, unfavorable equilibrium reaction 5, followed by the rapid reaction of the *M*'_i isomer (eq 9).

In the reactions of binuclear complexes of the type [X₅M–L–Ru^{III,II}(NH₃)₅]ⁿ, two different mechanistic patterns have been described in the literature.¹⁸ In the first one, which we call an R → M' ⇌ M → Ox scheme, a fully reduced (R) complex, e.g. [(edta)Ru^{II}–pz–Ru^{II}(NH₃)₅]³⁷ is oxidized by a one-electron process to the thermodynamically unstable electronic isomer, M', which is formed by attack of peroxydisulfate on the Ru^{II}(NH₃)₅ center, in a kinetically controlled reaction. Then, M' rapidly isomerizes via intramolecular electron transfer to M, the thermodynamically stable isomer; as the latter species has again a very reactive Ru^{II}(NH₃)₅ site, the complete oxidation to Ox is consummated. Our recent work on the [(NC)₅Fe–pyCN–Ru(NH₃)₅]ⁿ complexes shows that this type of mechanism is also operative.³⁸

On the other hand, the present work can be included in the alternative R → M ⇌ M' → Ox scheme. Here, the first one-electron product is the kinetically favored as well as the thermodynamically stable electronic isomer, M. The Ru^{II} site has a lower reduction potential than the Fe^{II} site, and besides, its reactivity toward peroxydisulfate is much higher, as already demonstrated in the reactions of the analog complexes with L = pz and bpa as bridging ligands.^{1,2} The conversion of M to Ox is now facilitated by the rapid isomerization to the unstable electronic isomer, M', which has again an available Ru^{II} site for the reaction proceeding to Ox. This was also observed in the bpa complex but not in the pz complex. Note that the unstable, reactive isomer in the imidazolate complex is in a much lower concentration than in the bpa complex (for the latter, *K*_{et} = 2.9 × 10^{–3})² but, on the other hand, reacts much faster because of its more favorable redox potential (see below). In a subtle balance, both factors determine the appearance of a more efficient process to the formation of Ox than the direct attack at the Fe^{II} site.

The significance of the measured second-order rate constant for the decay of M and the validity of the proposed mechanism, giving such a high value for *k*₉, can be nicely confirmed by including the data together with those obtained for other binuclear complexes, where the key process is the oxidation of a Ru^{II}(NH₃)₅ site by peroxydisulfate. By an assumption of ion-

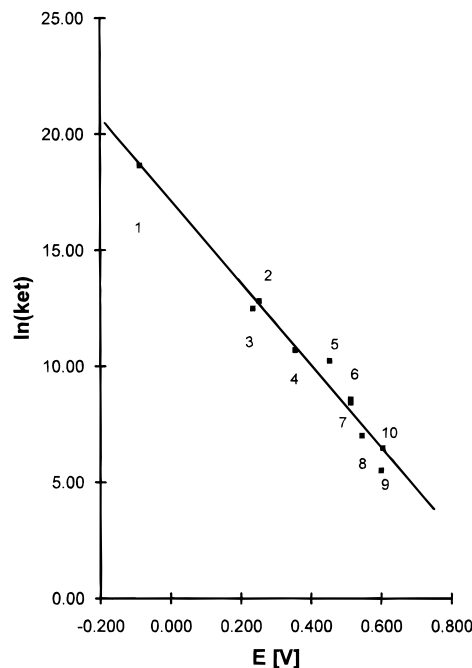
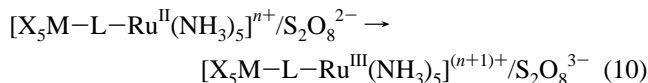


Figure 3. Plot of ln *k*_{et} vs *E*^o_{Ru} for “intramolecular” electron transfer in the ion pairs [X₅M–L–Ru^{II}(NH₃)₅]ⁿ⁺/S₂O₈^{2–}. The X₅M–L moieties are as detailed in Table 3 (*k*_{et} in s^{–1}, *E*^o_{Ru} in V vs NHE (both corrected for ion pairing, see text), *T* = 25.0 °C).

pair formation between the reactants, values of *k*_{et} for reaction 10 can be extracted from the kinetic data.



The relation between the free-energy change, Δ*G*^o₁₂ and the free energy of activation Δ*G*^{*}₁₂ of the outer-sphere electron-transfer reaction 10 is given by eq 11,³⁶ provided that (Δ*G*^o₁₂)²

$$\Delta G^*_{12} = (\Delta G^*_{11} + \Delta G^*_{22} + \Delta G^o_{12})/2 \quad (11)$$

≪ 8(Δ*G*^{*}₁₁ + Δ*G*^{*}₂₂). In eq 11, the subscript 12 refers to the cross reaction and 11 or 22 to the exchange reactions. The free energies are related to *k*_{et} according to eq 12, where *κ* is the electronic factor (equal to 1 for adiabatic reactions) and *ν*_n is a nuclear vibration frequency, taken to be 6 × 10¹² s^{–1}.²⁸

$$k_{et} = \kappa \nu_n \exp(-\Delta G^*_{12}/RT) \quad (12)$$

Since Δ*G*^o₁₂ = –*nF*(*E*^o₁₁ – *E*^o₂₂), a plot of ln *k*_{et} against *E*^o₂₂, the potential of the ruthenium couple in the binuclear

(37) Ram, M. S.; Haim, A. *Inorg. Chem.* **1991**, *30*, 1319.

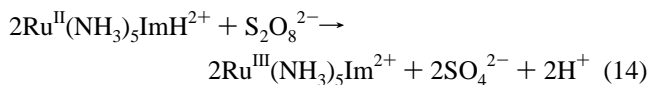
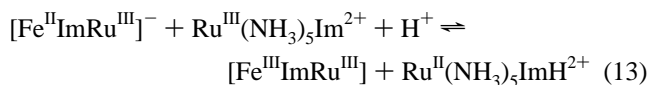
(38) Almaraz, A. E.; Gentil, L. A.; Baraldo, L. M.; Olabe, J. A. Submitted for publication.

complexes, should be linear with slope $-0.5/RT$ or -19.4 , provided that the reorganization free energies for the pentaammine–Ru(II) and –Ru(III) exchanges are insensitive to the identity of X_5ML .³⁶ By consideration of the data shown in Table 3, Figure 3 shows a slope of -17.8 , in reasonable agreement with theory. Note that the k_{et} values correspond to oxidation processes associated with either of the above mentioned mechanistic patterns.

In Figure 3, the k_{et} and E°_{Ru} values are taken from experimental data,^{36,39,40} with a correction for ion-pairing effects, as shown in Table 3. An extrapolation of the plot in Figure 3 for $E^\circ_{Ru} = -0.20$ V gives $k_{et} = 9.8 \times 10^8 \text{ M}^{-1} \text{ s}^{-1}$, thus explaining our inability to measure the one-electron oxidation process of the $[(NC)_5Fe^{II}-Im-Ru^{II}(NH_3)_5]^{2-}$ ion.

In the oxidation of M_i to O_i , we found that k_{nd} was sensitive to the concentration of the mononuclear $Ru^{III}(NH_3)_5Im^{2+}$ ion; in fact, the rate increased linearly with the concentration of added Ru(III). The results can be accommodated by proposing an intermolecular catalytic pathway, made available by the generation of mononuclear Ru(II) species, according to eqs 13 and 14.

The higher reactivity of Ru^{II} vs Fe^{II} in the reported binuclear systems is remarkable and relates not only to thermodynamic



driving forces or kinetic intrinsic factors. Even after corrections for the latter effects, Ru^{II} still reacts faster than Fe^{II} by a factor of about 10^2 . Two possible reasons were advanced, namely the nonadiabaticity in the reactions of $Fe^{II}(CN)_5L'^-$ with peroxydisulfate and the specific interactions arising between the latter species and the ammine ligands.¹⁸

Acknowledgment. Our thanks go to the Consejo Nacional de Investigaciones Científicas y Técnicas (CONICET), the University of Buenos Aires (UBA), and the Deutsche Gesellschaft für Technische Zusammenarbeit GmbH for economic funding. A.R.P. was a member of the Scholarships Program (UBA), and J.A.O. is a member of the research staff of CONICET.

Supporting Information Available: A figure showing the spec-troelectrochemical reduction of M_i (2 pages). Ordering information is given on any current masthead page.

IC951558O

(39) Miralles, A. J.; Armstrong, R. E.; Haim, A. *J. Am. Chem. Soc.* **1977**, *99*, 1416.

(40) Fürholz, U.; Haim, A. *Inorg. Chem.* **1987**, *26*, 3243.